The Laser calibration system for LHAASO-WFCTA

Y. Wang[1], L. Chen[1], H. Liu[1], Q.N. Sun[1], X. Li[1], J.J. Xia[1], F.R. Zhu[1], L.S. Geng[1], S.S. Zhang[2] and Y. Zhang[2] on behalf of the LHAASO Collaboration

1. School of Physical Science and Technology , Southwest Jiaotong University, Chengdu 611756, China

2. Key Laboratory of Particle Astrophysics, Institute of High Energy Physics of the Chinese Academy of Sciences, Beijing 100049, China

ONLINE ICRC 2021 THE ASTROPARTICLE PHYSICS CONFERENCE Berlin | Germany 37th International Cosmic Ray Conference 12–23 July 2021

The Wide Field-of-view Cherenkov Telescope Array (WFCTA) of Large High Altitude Air Shower Observatory (LHAASO) is designed to measure the Cherenkov and fluorescent light created in the extensive air showers by cosmic rays (CRs) from ~30 TeV to several EeV. In order to achieve an end-to-end calibration method for WFCTA, three Laser lidar facilities have been installed at LHAASO. They feature two N_2 and one YAG Lasers which direct calibrated and pulsed beams into sky. Light scattered from Laser beams produces tracks recorded by the telescope detectors. The Laser calibration systems are used to investigate properties of the atmosphere and air fluorescence. We introduce the design and performance of the Laser facilities at LHAASO. After excluding the inconsistency of all SiPMs of the telescope, we find that the experimental data of the images collected by telescopes agree noticeably well with Monte Carlo's simulation.

1. Introduction

LHAASO consists of three interconnected arrays of—the Water Cherenkov Detector Array (WCDA), Kilometer Square Array (KM2A) and Wide Field-of-view Cherenkov Telescope Array (WFCTA). LHAASO is located at 4,410 m above sea level in Haizi Mountain, Sichuan Province, China [1，2]. The WFCTA is designed to measure the Cherenkov and fluorescent light created in the extensive air showers by cosmic rays from ~30 TeV to several EeV. The energy spectra of cosmic rays measured by WFCTA are mainly obtained by calculating the number of photons detected by the telescope. As a result, it is necessary to achieve an end-to-end calibration method to the number of photons, considering the overall conversion factor from analog-to-digital converter (ADC) counts to the light flux at the telescope entrance. Cherenkov light is partially lost due to the scattering by air molecules (Rayleigh scattering) and aerosols (Mie scattering) when propagating in air [3, 4]. The key point in CR energy spectra measurement is the determination of the total energy of reconstructed air showers as it requires an absolute calibration for the detector [5]. The Laser calibration system (LCS) is adopted to detect the atmospheric fluorescence (Cherenkov light). Based upon the light flux calculation at the front of the detector, one can straightly calibrate the detector by analyzing the measured ADC counts [6]. For the WFCTA project, in response to various needs, 3 sets of Laser calibration and atmospheric monitoring systems have been built at LHAASO, as demonstrated in Figure 1. The principle of the absolute calibration of photons for a telescope is as follows: a laser pulse with a certain energy and polarization is emitted from the calibration room to the field of view (FoV) of the telescope at a specific angle with a time delay during a period of time (see Fig. 2). By the calculation of the expected and the acquired light fluxes at the front of the aperture of the telescope, it is attainable to calibrate the number of photons from a Cherenkov light.

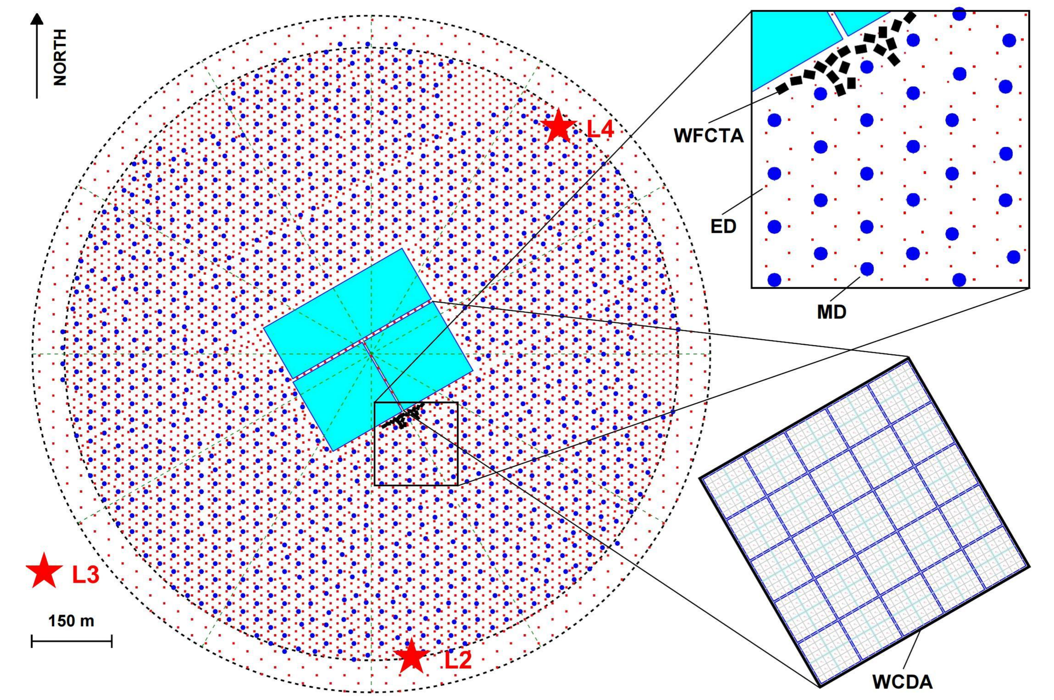

Figure 1: The schematic layout of LHAASO. The location of each LCS is indicated by a red star (L2, L3 and L4).

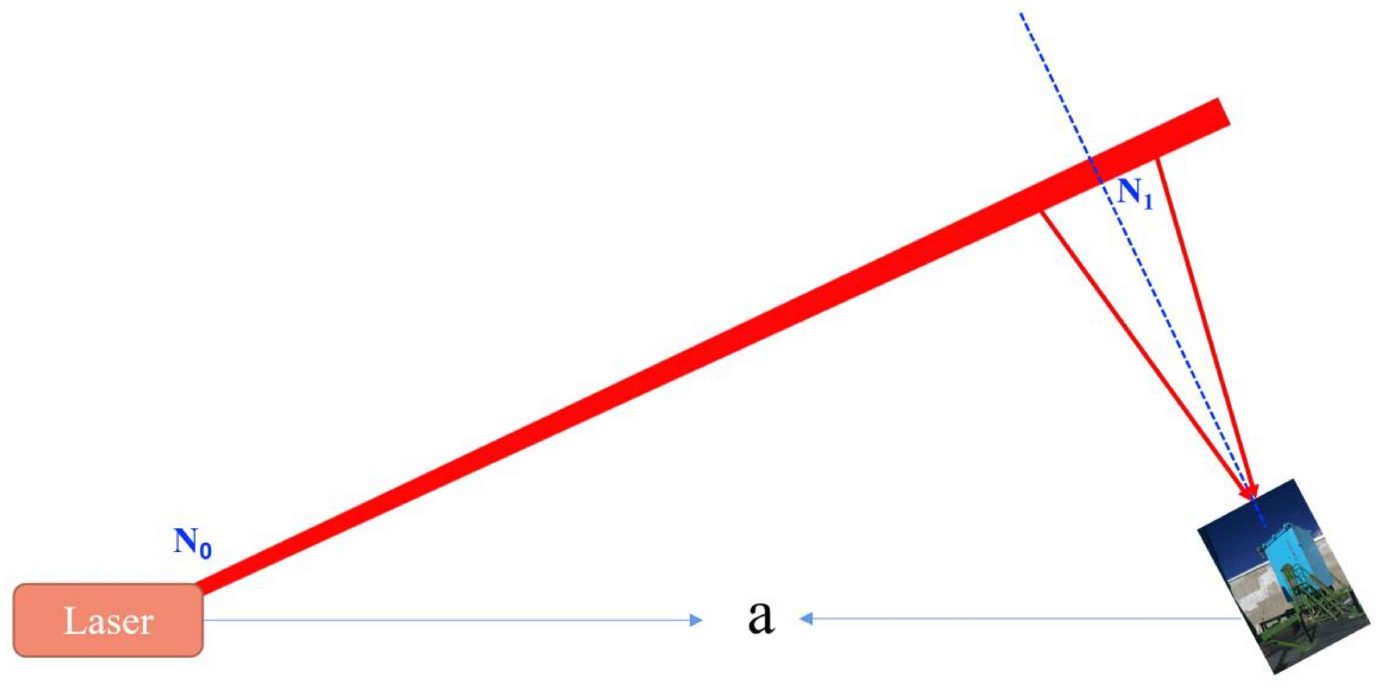

Figure 2: The schematic diagram of Laser calibration. N_0 and N_1 are the number of photons emitted into atmosphere and scattered into the telescope, respectively, and a is the distance between a Laser and the telescop.

2. Laser calibration system

The LCS of WFCTA is generally composed of two parts: hardware and software for controlling, including a Laser head and its controller, a calibration room, the cruise control and imaging system. The L2 is 465 m, L3 is 1075 m and L4 is 650 m from the telescope array, respectively.

2.1 N_2 Laser facility

The layout of L2 is depicted in Figure 3. It mainly consists of six parts, including a computer controlling system, a mechanical system, a temperature controlling system, a timing system, a monitoring system and a nitrogen Laser. A programmable logic controller (PLC) is used to precisely and remotely control the accuracy of the Laser beam pointing through a high-precision rotating and lifting platform. The measurement shows the angular and lifting accuracy of the mechanical platform is better than 0.004° and 0.075 mm, respectively. In addition, the corresponding repeatability of this platform is better than 0.003° and 0.025 mm, respectively. All of these parameters permits a stable and accurate pointing of the Laser beam into sky. The heart of the system is a nitrogen Laser (NL100), which produces a circularly polarized beam. It is triggered by the GPS signal and provides 3.5 ns pulses at 337 nm, with a repetition rates of 1 Hz. The pulse energy is up to 170 μJ.

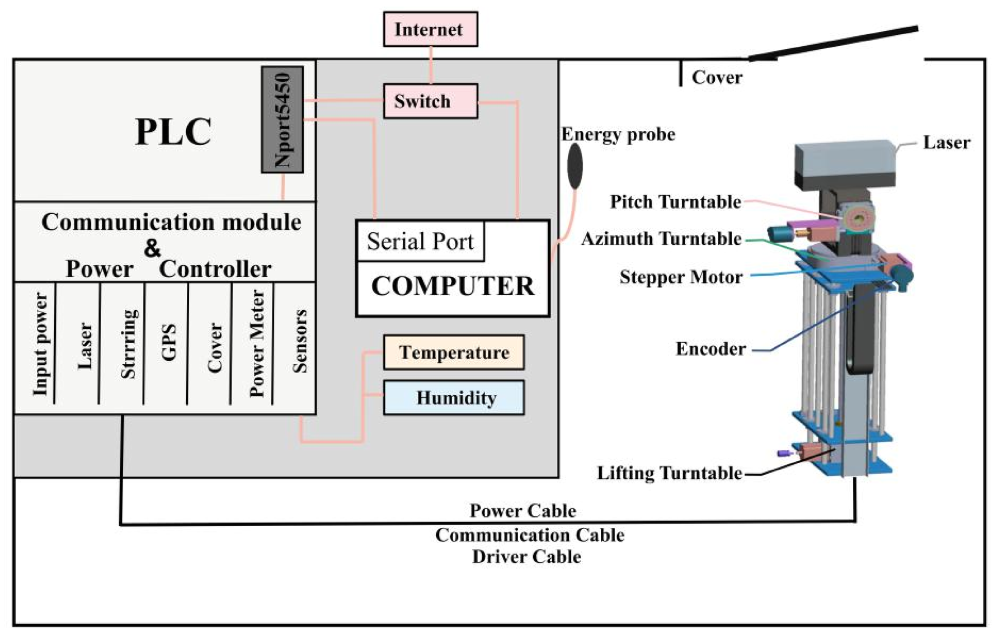

Figure 3: Schematic diagram of the L2 N_2 Laser facility.

2.2 YAG Laser facility

A frequency tripled Nd: YAG Laser was set up at the site of L3, which produces a vertically and linearly polarized beam of 355 nm. The beam is pulsed, with a width of 7 ns, and a maximum energy per pulse of 2 mJ. A quarter-wave plate was brought in to the beam path and a phaseshift was added to convert the linear polarization into a circular one. An error less that 5% is feasible for the calibration of the photon number. To accurately monitor and measure each Laser pulse to minimize the error attributed to the energy fluctuation, a beam splitter was added in the beam path and reflected ~ 40% of the beam (reference beam) into an energy detector. The energy ratio for them is independent of the emitted laser pulse energy and only committed to the angle of incidence and the polarization of the beam. The fluctuation of the emitted light cancels out and it paves the way to a pulse-by-pulse energy monitoring by recording the pulse energy of the reference beam.

3. Experimental and simulated data.

Eighteen wide field of view Cherenkov telescopes were installed surveying the sky above the whole array with a coverage of 4608 square degrees. Each Laser acquires external trigger signals with different delays, intending to distinguish tracks from different Laser systems. Two images detected by a telescope of WFCTA for a nitrogen Laser event and a YAG Laser event, respectively, are shown in Figure 4. Each Laser acquires external trigger signals with different delays, intending to distinguish tracks from different Laser systems. The number of photon-electron (Npe) of nitrogen Laser event detected by one telescope is shown in Figure 5 to study the effect of the temperature on LCS. After the correction of temperature on Npe (based on a carefully designed LED system), the mean Npe is a constant as temperature varies. Moreover, the fluctuations of Npe are very similar to that of the pulse energy, which means that the fluctuation introduced by the Laser energy instability is considerably small. A dedicated program based on Monte Carlo method was developed to simulate the LCS, including the properties of the following parameters: the Laser (the energy, polarization, beam size and divergence, etc.) and the rotating and lifting platform (the absolute zero direction and the elevation angle of the rotating axis, etc). The Mie scattering in the atmosphere and the simulation inside the telescope (the same one for the CR simulation) are also involved. Currently the US standard model is applied to the simulation, and other atmosphere models are also optional. Figure 6 illustrates the comparison of the experimental data of the images collected by telescopes with the Monte Carlo simulated events, which agrees well. Detailed studies on the gain of the telescope and aerosol measurement are ongoing.

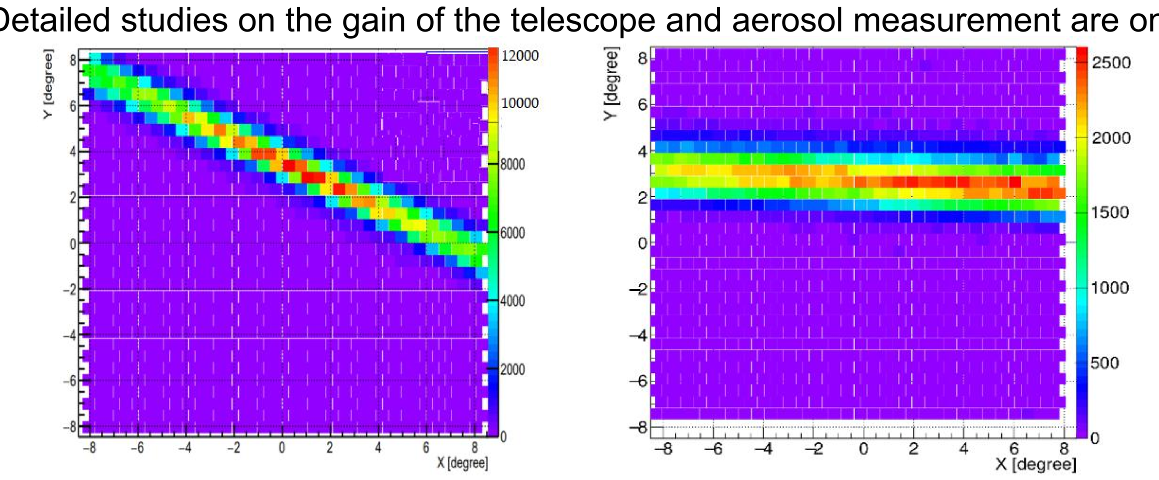

Figure 4: The images detected by a telescope of WFCTA for a nitrogen Laser event (left) and a YAG Laser event (right).

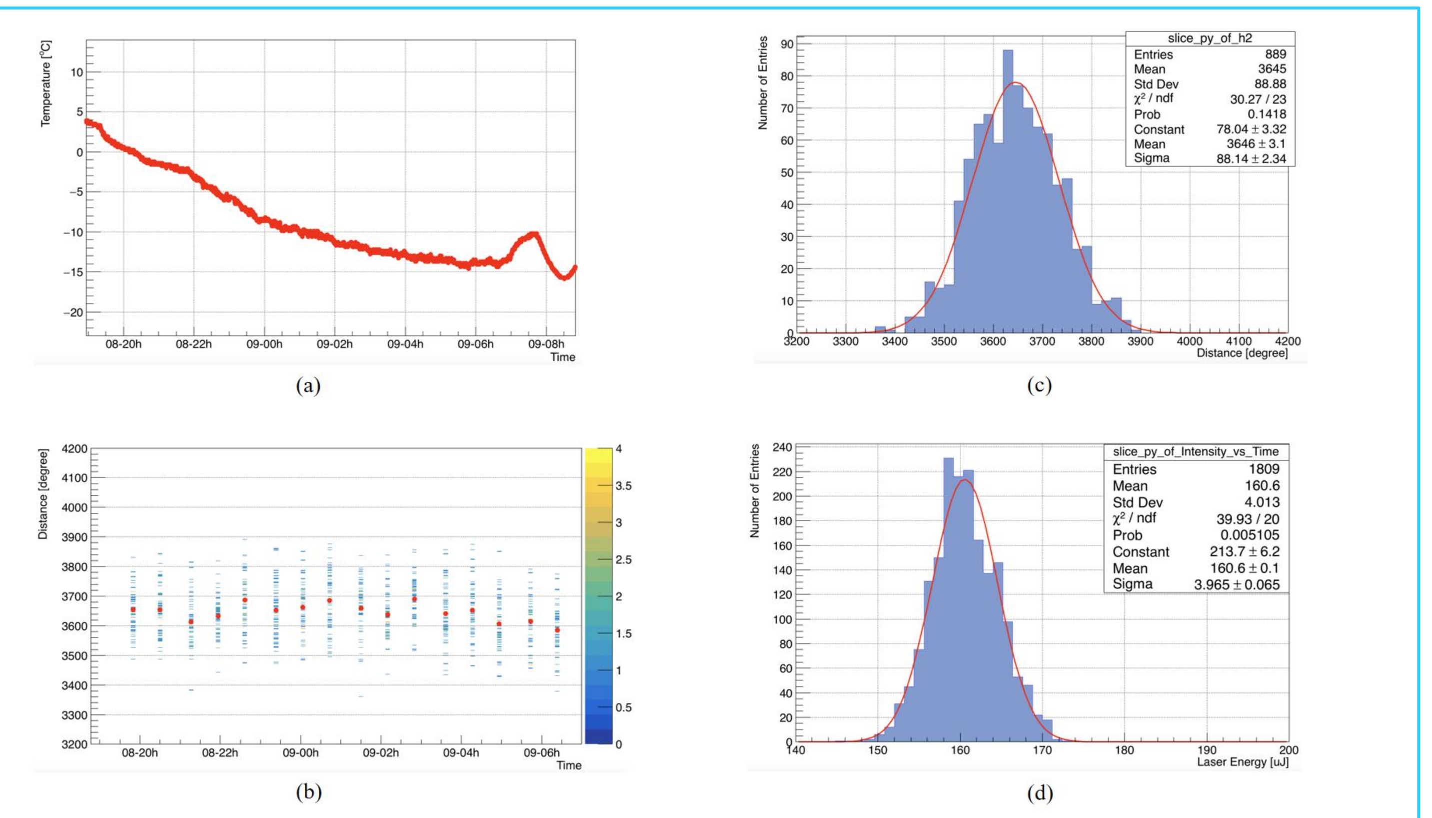

Figure 5: Left: Temperature vs Time (a) and Npe vs Time (b); Right: distribution of the Npe (c) and distribution of laser energy (d).

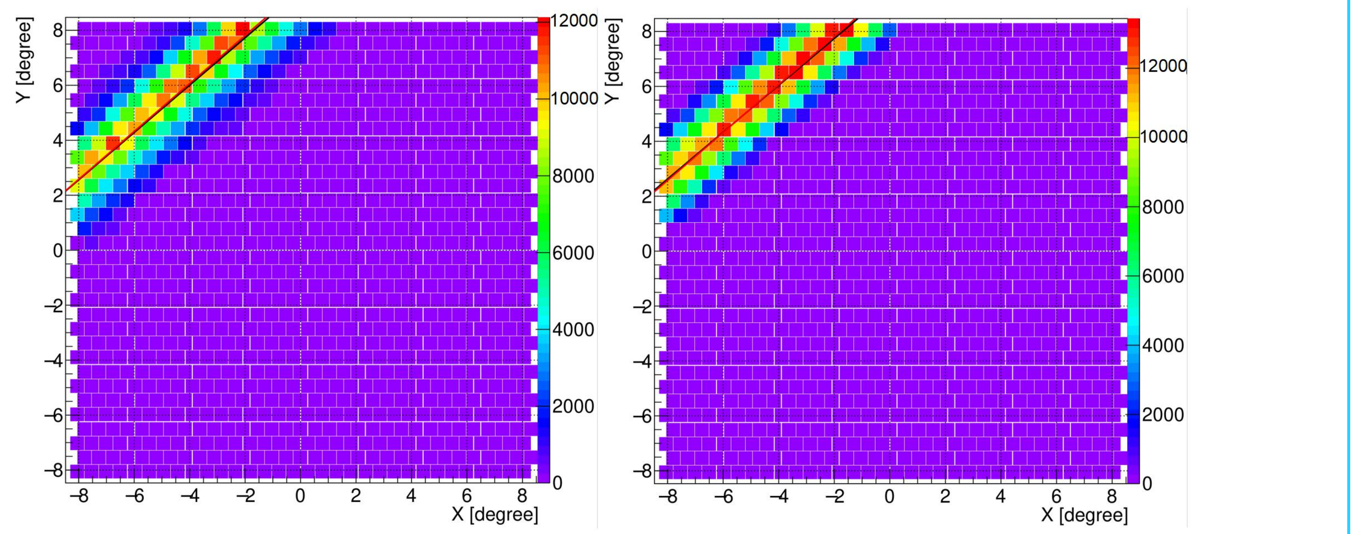

Figure 6: The image of one Laser event detected by one telescope of WFCTA. Left: experimental data; Right: Monte Carlo simulated event. The black line is a linear fit for the image, and the red line is the predicted position of the image based on the calculation with the astronomical package slalib, which is the same for the plots both on the left and right.

Acknowledgement

This work is supported in China by the Fundamental Research Funds for the Central Universities (grant numbers 2682020CX77, 2682020CX73, 2682020CX74). It is also supported by the Science and Technology Department of Sichuan Province (grant numbers 2021YFSY0031, 2020YFSY0016), and by NSFC (grant number 11947404), and by National Key R&D program of China (grant number 2018YFA0404201).

Reference

[1] Cao, Z., Aharonian, F.A., An, Q. *et al.*, *Ultrahigh-energy photons up to 1.4 petaelectronvolts from 12 γ-ray Galactic sources*, Nature 594, 33–36 (2021).

[2] Cao, Z, *A future project at Tibet: the large high altitude air shower observatory (LHAASO)*, Chin. Phys C 34, 249–252 (2010).

[3] G. Placzek, The Rayleigh and Raman Scattering, Lawrence Radiation Laboratory (1959).

[4] G. Mie, *Contributions to the optics of turbid media, particularly of colloidal metal solutions*, Ann. Phys 25 (3), 377–445 (1908).

[5] F. Aharonian, Q. An, Axikegu, L. X. Bai, Y. X. Bai, Y. W. Bao, D. Bastieri, X. J. Bi, Y. J. Bi, H. Cai *et al.*, *Calibration of the Air Shower Energy Scale of the Water and Air Cherenkov Techniques in the LHAASO experiment*, [arXiv:2104.04965 [astro-ph.IM]] (2020).

[6] A. Konopelkoa *et al.*, *Properties and performance of two wide field of view Cherenkov/fluorescence telescope array prototypes*, Nuclear Inst. and Methods in Physics Research, A 629, 57–65 (2011)